

Suitability of Quaternary Sediments of Wadi Arar, Saudi Arabia, as Construction Materials

An Environmental Radioactivity Approach

Mohammed A. M. Alghamdi

Faculty of Earth Science,
King Abdulaziz University,
Jeddah, Saudi Arabia
mmushrif@kau.edu.sa

Abstract—The surficial quaternary deposits of Wadi Arar were radioactively evaluated for construction purposes. The concentrations of ^{226}Ra , ^{232}Th , and ^{40}K were used to evaluate the radioactive suitability of Wadi Arar. Gamma-spectrometry technique with an HPGe detector was used to measure the concentrations of Ra, Th, and K. The average specific activities of Ra, Th, and K were 22.92, 16.99, and 223.66Bq/kg respectively. The average value of the air absorbed dose rate (D) was 30.47nGy/h. The average values of the indoor and outdoor annual effective dose equivalent (AEDE) were 149.46 and 37.36 $\mu\text{Sv/y}$ respectively. The average value of the radium equivalent activity index (Ra_{eq}) was 64.44Bq/kg. The maximum values of the external and internal hazard index (H) were 0.20 and 0.27 respectively. Radioactivity concentration and hazard index values are within the acceptable global values and do not pose any significant radiological threat to the population. These results reflect the safety of Wadi Arar as a site for construction and the potential to use depositional sediments at the site as construction materials.

Keywords—environmental; geology; construction; radiation; HPGe

I. INTRODUCTION

Wadis, coasts, and deserts are possible construction sites and sources for construction materials. Radioactive hazards are one of the factors that affect the selection of construction material sites. Geological, geochemical, pathological, and ecological processes along with seasonal changes are some of the main processes that influence natural radioactivity [1]. Radiation level concentrations differ depending on rock-type, soil, or sediment [2]. The discharge of gamma radiation from naturally occurring radioisotopes depends on land conditions, and is globally characterized by various levels [3]. Due to the presence of active faults and lineaments, some areas experience elevated concentrations of K, Ra, and Th in soil samples [4]. Similar researches concluded in varying results. Gamma-ray spectroscopy was used to assess the average effective dose of ^{226}Ra , ^{232}Th , and ^{40}K in Punjab, India in [5]. Assessments of the natural radionuclide contents of ^{238}U , ^{232}Th , and ^{40}K at Tushki, Egypt using gamma-spectrometry analysis showed high

background radiation, thankfully far from habitation and cultivated regions [6]. Naturally occurring radioactivity in soil samples at Akwa Ibom, which were evaluated were less than the recommended safety limits [7]. All health hazard indices were well below their recommended limits for samples collected from locations at Aden, south of Yemen [8]. Maximum and minimum activity ^{40}K concentrations of sediments in water samples at Abuja, Nigeria were ranked in [9]. Soil sediments in the Udi and Ezeagu areas of the Enugu State, Nigeria have reduced concentrations of ^{40}K , ^{226}Ra , and ^{232}Th [10]. Authors in [11] found that the radiological effects of soil samples from Geregu were below the standard limits and posed no potential significant effects on public health. Authors in [2] analyzed the radionuclide activity concentrations of ^{40}K , ^{226}Ra , and ^{232}Th in sand deposits from the Bharathapuzha River, India, and found that the concentrations were higher than the international recommended values. The specific natural radionuclide activities in sediment samples collected from Beni Haroun Dam, Algeria had no hazardous indices compared with analog measurements from other locations [12].

In Saudi Arabia, the strategic road that connects Arar and Aljouf is crossing Wadi Arar while the urban expansion of Arar extends in the southeastern direction towards Wadi Arar (Figure 1). Radon concentrations in this Wadi, reflect a significant correlation between the RAD7 and Cr-39 techniques that were used to detect it [14], while it has a significant correlation with coarse and fine sand grain size [15]. Authors in [16-19] used gamma spectroscopic analysis measuring the radioactivity of Ra, Th, and K, to obtain hazard indices in AlKhobar, Jeddah, Aqabah, and Ad-Dahna respectively. According to them, the hazard indices at Ad-Dahna were below the global average value, but the values of K at Jeddah and Aqabah were higher than the global average.

Considering ^{226}Ra , ^{232}Th , and ^{40}K , this study was conducted on 22km of the surficial deposits of Wadi Arar (Figure 1). The assessment of radiation concentrations and hazard indices at this Wadi will allow us to i) evaluate the site validity for future urbanization and the potential use of sediment deposits as construction materials, ii) support interpretations of subsurface structural geology, and iii) perform comparisons and

Corresponding author: Mohammed A. M. Alghamdi

interpretations of radiation hazards in Wadi environments with the global environment.

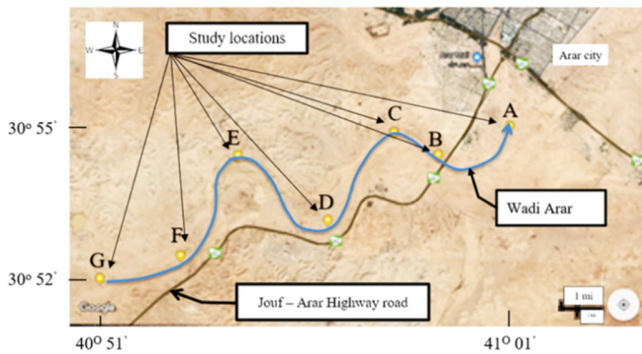


Fig. 1. Study area profiles in Wadi Arar. (Screenshot from Google Earth [13], © 2018 Google, Image © 2019 Maxar Technologies, Image © 2019 CNES/Airbus)

II. STUDY AREA

A. Geological Setting

The Arar quadrangle underlies the Late Cretaceous Aruma Formation and Paleogene and Neogene sedimentary rocks [20]. Sedimentary rock units of Devonian, Silurian, and Ordovician are also representative of the subsurface formations. Wadi Arar cuts off these formations from the southwest to the northeast, filling this area with quaternary deposits, such as gravel, sand, and silt, which lie above the sedimentary rocks. According to the structural geology perspective, the Arar arch traverses the study area, trending from southwest to northeast. Flood seasons have continually transported these deposits and soil sediments on the same trend of Arar arch.

B. Location and Sampling

Geological and topographic maps of the northern border region [13, 20] were used to adapt to the study area. The study area of Wadi Arar is located between 30°50'30"N and 30°56'30"N and 40°50'30"E and 41°02'30"E. Seven profiles (A, B, C, D, E, F, and G) were chosen at the peak of water deposition or sediment erosion. The total distance from profile A to G was 22km, with an average distance of 3km between each profile (Figure 1). Five samples of 1kg from each station were sealed in plastic bags and stored for laboratory tests.

III. HAZARD PARAMETERS

A. Detector

Samples with an average weight of 180g were placed in sealed cylindrical 100mL plastic containers and used to measure the Naturally Occurring Radioactive Materials (NORM). The containers were stored for one month to obtain secular equilibrium in each natural radioactive series, where the rate of daughter decay reaches equilibrium with that of the parents. Activity concentration measurements were performed using a gamma-ray spectrometer equipped with a high-purity germanium (HPGe) detector that was enclosed in a 10cm cylindrical multilayer graded shield (Canberra 747E). The

HPGe detector has an efficiency of 60% and energy resolution of 2.4keV at 1,332.5keV from a ^{60}Co gamma-ray. The detector was coupled with an amplifier to the computer using a multi-channel analyzer. Calibration of the energy, efficiency of the detector and efficiency of the sample geometry were performed using the methods described in [21–23]. 1,461 keV γ -line was used to determine ^{40}K activity while ^{226}Ra and ^{232}Th activities were determined indirectly using the most intense non-interfering gamma lines (295 and 352keV for ^{214}Pb , 609, 1120, and 1764keV for ^{214}Bi , 583 and 2614keV for ^{208}Tl , 338, 911, and 968keV for ^{228}Ac). Each sample was measured for 24hr in order to obtain a sufficient amount of data [24].

B. Air-Absorbed Dose Rate (D)

The measured concentrations of ^{226}Ra , ^{232}Th , and ^{40}K were converted to a total absorbed gamma dose rate in the air at one meter above the ground using the Monte Carlo method [3] based on the following equation:

$$D(\text{nGy} \cdot \text{h}^{-1}) = 0.462A_{\text{Ra}} + 0.621A_{\text{Th}} + 0.0417A_{\text{K}} \quad (1)$$

where D is the air-absorbed dose rate and A_{Ra} , A_{Th} , and A_{K} are the activities, in Bq/kg, of Ra, Th, and K, respectively.

C. Annual Effective Dose Equivalent (AEDE)

The annual effective dose provides a measure of the total radiation risk to an individual organism. The conversion coefficient from the absorbed dose in the air to the effective dose and the indoor occupancy factor was used to estimate the annual effective dose with a conversion factor of 0.7Sv/Gy [2]. Assuming that people spend, on average, approximately 20% of their time outdoors and 80% indoors [3], the annual effective dose was calculated with the following equations:

$$\text{AEDE indoor (mSv } \text{y}^{-1}) = D(\text{nGy} \cdot \text{h}^{-1}) \times 8760 \text{ h} \times 0.8 \times 0.7 \text{ Sv Gy}^{-1} \times 10^{-6} \quad (2)$$

$$\text{AEDE outdoor (mSv } \text{y}^{-1}) = D(\text{nGy} \cdot \text{h}^{-1}) \times 8760 \text{ h} \times 0.2 \times 0.7 \text{ Sv Gy}^{-1} \times 10^{-6} \quad (3)$$

D. γ -Ray Radiation Hazard Indexes (Ra_{eq})

The natural radiation in building materials is not uniform and is typically determined by the concentrations of ^{226}Ra , ^{232}Th , and ^{40}K [2]. Uniformity for radiation is denoted in terms of radium equivalent activity Ra_{eq} , in Bq/kg, to match the specific activity of a fabric that contains a different quantity of ^{226}Ra , ^{232}Th , and ^{40}K by a single amount. It is a commonly used hazard index, which is calculated using the following equation [2]:

$$Ra_{\text{eq}} = C_{\text{Ra}} + 1.43 C_{\text{Th}} + 0.077C_{\text{K}} \quad (4)$$

where C_{Ra} , C_{Th} , and C_{K} are the activity concentrations of ^{226}Ra , ^{232}Th , and ^{40}K , in Bq/kg respectively. It has been assumed that 370Bq/kg of ^{226}Ra , 259Bq/kg of ^{232}Th , or 4810Bq/kg of ^{40}K produce the same gamma dose rate [2].

E. Hazard Index (H_{ex} , H_{in})

In their research on sandy soil, authors in [24] obtained an external hazard index using the Ra_{eq} expression from (4) by

suggesting that the maximum allowed value (equal to unity) corresponds to the upper limit of Ra_{eq} (370Bq/kg). This index value must be less than unity to maintain an insignificant level of radiation hazard, i.e. the radiation exposure due to construction material radioactivity is limited to 1.0mSv/y. The external hazard index can be defined with the following equation:

$$H_{ex} = \left(\frac{A_{Ra}}{370} + \frac{A_{Th}}{259} + \frac{A_K}{4810} \right) \leq 1 \quad (5)$$

where A_{Ra} , A_{Th} , and A_K are the specific activities of Ra, Th, and K in Bq/kg respectively, while 370, 259 and, 4810 are the activities, in Bq/kg, of Ra, Th, and K that produce the same gamma dose rate.

In addition to the external hazard index, radon and its short-lived daughter products are hazardous to respiratory organs [3].

Internal exposure to radon and its daughter products can be quantified with the internal hazard index H_{in} [3], which is given by the following equation:

$$H_{in} = \left(\frac{A_{Ra}}{185} + \frac{A_{Th}}{259} + \frac{A_K}{4810} \right) \leq 1 \quad (6)$$

where 185, 259 and, 4810 are the activities of Ra, Th, and K respectively that produce the same gamma dose rate. The value of the internal hazard index H_{in} must be less than unity to maintain a negligible level of radiation hazard [25].

IV. RESULTS

The concentrations of the naturally radioactive elements (K, Ra, and Th) and the hazard indices from soil sediments in the surficial layer at different locations of the Wadi Arar are listed in Table I and plotted in Figures 2–7.

TABLE I. NATURAL RADIONUCLIDE ACTIVITY LEVELS AND RADIATION RISK INDICES.

Location	Indice	²²⁶ Ra	²³² Th	⁴⁰ K	D	AEDE indoors	AEDE outdoors	Ra_{eq}	H_{ex}	H_{in}
	Unit	Bq/kg	Bq/kg	Bq/kg	nGy/h	μSv/y	μSv/y	Bq/kg		
A		19.80	8.56	132.89	20.00	98.14	24.53	42.27	0.11	0.17
B		21.85	16.59	260.00	31.24	153.25	38.31	65.59	0.18	0.24
C		20.79	18.89	305.96	34.09	167.25	41.81	71.36	0.19	0.25
D		22.59	17.16	169.20	28.15	138.09	34.52	60.16	0.16	0.22
E		26.20	20.13	241.95	34.69	170.20	42.55	73.62	0.20	0.27
F		25.93	19.13	265.30	34.92	171.32	42.83	73.71	0.20	0.27
G		23.31	18.45	190.30	30.16	147.96	36.99	64.35	0.17	0.24
Average		22.92	16.99	223.66	30.47	149.46	37.36	64.44	0.17	0.24
Max. allowable value [2]		35	30	400	57	450	70	370	≤1	≤1

The average concentrations of Ra, Th, and K at Wadi Arar are 22.9, 17.0, and 223.7Bq/kg respectively, while the value range was 19.8–26.2 for Ra, 8.56–20.13 for Th and 132.89–305.96 for K. It was observed that $K > Ra > Th$ which is consistent with their global order while the average concentrations of Ra, Th, and K were lower than the average internationally recommended concentrations of 35, 30, and 400 respectively [3]. Th and K were 0.6 times lower than the average internationally recommended values, whereas Ra was 0.7 times lower. Depending on the similarity between the three radioactive isotopes at each location, data were plotted using a 3-D method to classify the Wadi Arar from a radioactivity cluster perspective (Figure 3). Wadi Arar was classified into three clusters: the first cluster included profiles A, D, and G, the second included profiles C and B, and the third included profiles E and F.

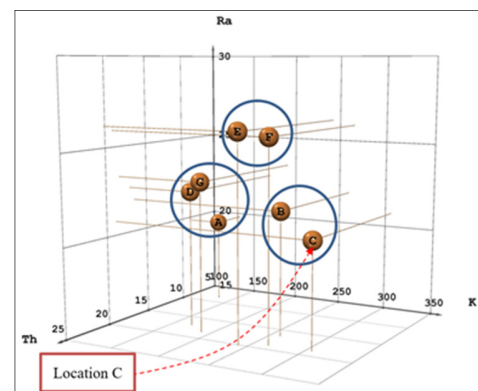


Fig. 3. A 3-D plot of the Ra, Th, and K concentrations (Bq/kg) for the different study area profiles

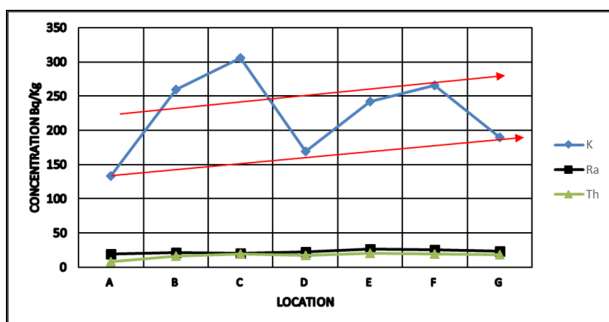


Fig. 2. Ra, Th, and K concentrations at the Wadi Arar which show a generally increasing trend in K concentration (red arrows)

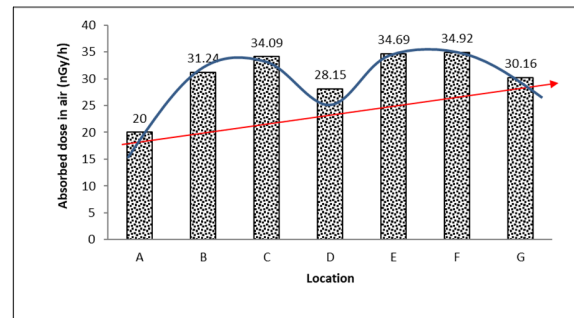


Fig. 4. The absorbed dose in air which shows a generally increasing trend in concentration (red arrow)

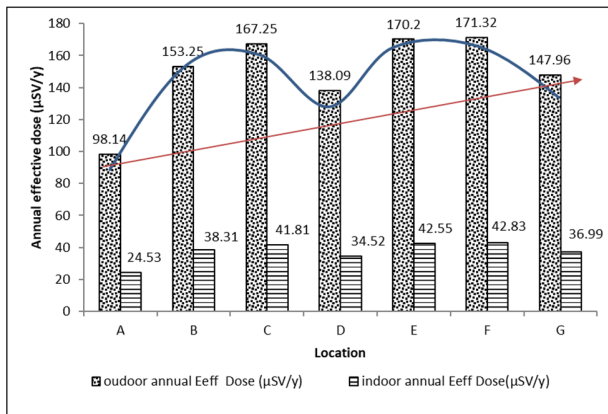


Fig. 5. The annual indoor and outdoor effective dose. Doses are characterized by a generally increasing trend (red arrow)

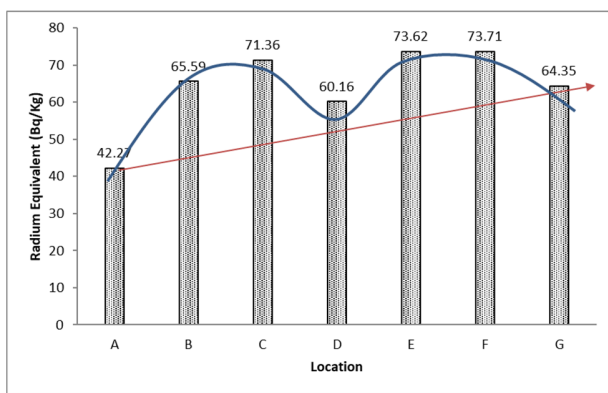


Fig. 6. The radium equivalent activity Ra_{eq} showing a generally increasing trend (red arrow)

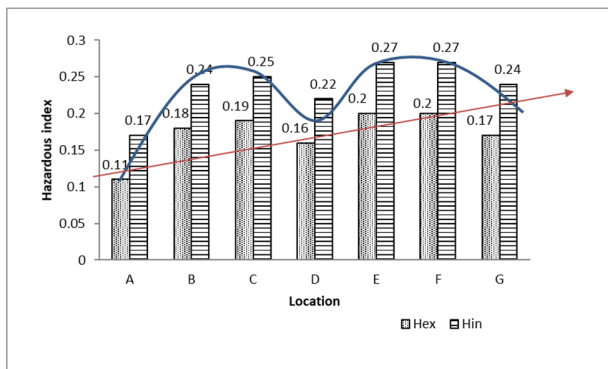


Fig. 7. Internal and external hazard indices characterized by a generally increasing trend (red arrow)

Assuming that the naturally occurring radionuclides have a uniform distribution [3], the absorbed dose rates (D) were calculated from the gamma radiation in the air at 1m above the ground. The rates varied from 20 to 34.92nGy/hr, with an average value of 30.47nGy/hr (Table I). Figure 4 shows two peaks of the D values at stations C and F. The D values increase from the northeast (location A) to the southwest (Location G) (red arrow). Based on these results, the Wadi Arar can be classified into two absorbed dose zones, i.e. A–D and D–G. The calculated values for AEDE were between 98.14 and

171.32µSv/y, with an average of 149.46µSv/y. The annual effective outdoor dose rate ranges from 24.53 to 42.83µSv/y, with an average of 37.36µSv/y (Table I). Figure 5 shows the changes in both indoor and outdoor annual effective dose, which are characterized by a general trend (red arrow) that increased from location A to G with two peaks at C and F. Table I also summarizes the Ra_{eq} estimated values for the study area. Figure 6 shows the changes that occur at each location, which are characterized by a general trend that increases from A to G with two peaks at C and F. The calculated values for the external and internal hazard index (H_{ex} and H_{in}) ranged from 0.11 to 0.20 and 0.17 to 0.27 respectively. Figure 7 illustrates those changes, which are characterized by a general hazard index trend (red arrow) that increases in the southwest direction (location D). Based on the results for both isotope concentrations and hazard indices, two radioactive zones can be assessed. The values increase from the northeast to the southeast and are lower than average global values.

V. DISCUSSION

It was observed that, the values at profile D were less than the international average for a gamma radiation dose level from terrestrial sources [3] and less than the average value reported by numerous countries such as the United States, Switzerland, Spain, Greece, Egypt, Iran, India, China, and Korea in 2005 [4]. The results for the indoor and outdoor AEDE were within the average global limits, which are 450 and 70µSv/y, respectively. Therefore the sampled sediments can be safely used for construction materials. The estimated average Ra_{eq} value was lower than the maximum permissible value of 370Bq/kg suggested for building materials concerning radiation hazards [2]. H_{ex} and H_{in} values were lower than unity, so the soil samples at Wadi Arar are considered safe and can be used as construction materials without posing any significant radiological threat to the population, according to [26]. The concentrations of radioactive elements generally increase from the northeast to southwest. In comparison with ^{232}Th and ^{226}Ra , ^{40}K has the highest radioactive concentrations throughout Wadi Arar, which includes two concentration peaks at profiles C and F (Figure 2), indicative of the availability of potash feldspar minerals. Fluctuations in the radioactive concentrations may represent the availability of more rock and mineral resources in the study area, such as carbonate and silicate minerals that include sedimentary rocks from the Badanh and Zallum formations, i.e. limestone, sandstone, and shale [20, 27].

Based on a similarity analysis, Figure 2 shows profiles A, D, and G as one cluster, which has reduced ^{40}K concentrations, whereas profiles E and F represent another cluster that has increased ^{226}Ra concentrations. Profiles B and C have the highest ^{40}K concentrations. The availability of more Sha'ibs [28] or tributaries that pass through profiles A, D, and G possibly transport new sediment to wadi deposits may reduce the isotope radiation concentration. Additional sediments modify the deposit composition by adding new minerals. On the other hand, the proximity of geological structures, such as the Arar arch folds or graben faults, possibly changes radioactive element concentrations (Figure 8). For example, weathering and erosion can affect the fold's hinge zone and cover it with sediments. Profiles A, D, and G are located on

identical rock types, where profile A is located on the first fold limb, D is located on the second fold limb, and G is on the third fold limb. These locations may create a situation that yields identical radioactive concentrations at a small-scale. Background radiation is present everywhere so, spectrum analysis should be conducted using lead absorbers around the instruments. Otherwise high temperature can create electrical noise and ruin the detector, so the detector must be cooled.

From a radiation perspective, local authorities have to take the conclusions of this paper in consideration along with the construction codes in Wadi Arar. The results of this study on the radioactivity in Wadi Arar can be used for global comparison and mapping. This requires essential communication between the construction sector and the population regarding the radiation issues in Wadi Arar.

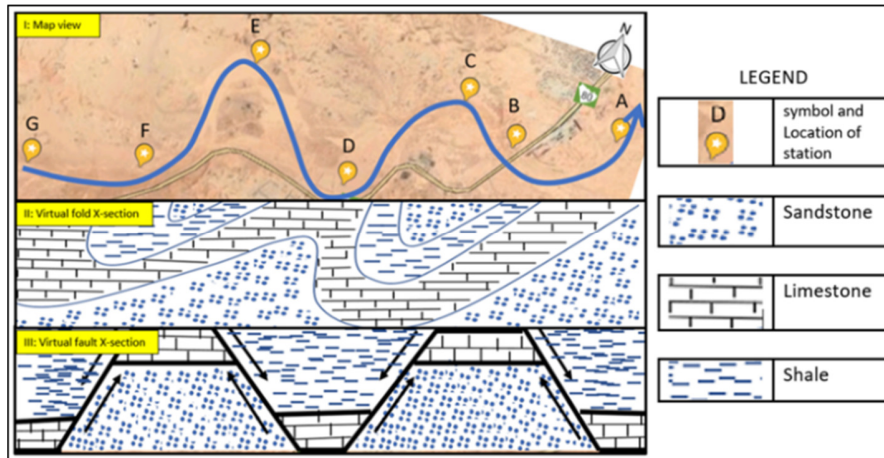


Fig. 8. I: A map view of the study area, II: A virtual fold cross-section, and III: A virtual fault cross-section

VI. CONCLUSION

Based on the acquired results from this study on the radioactivity of ^{226}Ra , ^{232}Th , and ^{40}K in Wadi Arar, the following can be concluded:

- The average radioactivity concentrations of ^{226}Ra , ^{232}Th , and ^{40}K of the soil surface deposits in Wadi Arar are 22.92, 16.99, and 223.66Bq/kg respectively, while their range is 19.8–26.2, 8.56–20.12, and 132.89–305.96Bq/Kg, respectively.
- Radioactivity tends to increase from the northeast to southwest.
- Based on the fluctuations in radioactivity, Wadi Arar deposits can be divided into two radiological zones: from locations A to D and from D to G with maximum concentrations of 365 and 265Bq/Kg, respectively.
- From a radiological perspective and regardless of other geotechnical properties, soil surface deposits in Wadi Arar can be used as construction materials without posing any significant radiological threat.
- Potassium has higher concentration compared with the two other radioactive elements, which indicates high occurrence rate of potash feldspar minerals in Wadi Arar deposits, such as plagioclase.
- Fluctuations in radioactive concentrations in Wadi Arar may reflect the occurrence of geological structures, such as fault, folds, or changes in lithology.

ACKNOWLEDGEMENT

This work was supported by the Deanship of Scientific Research, Northern Border University, Saudi Arabia, under the Grant No 45/2001.

REFERENCES

- [1] L. Guagliardi, N. Rovella, C. Apollaro, A. Bloise, R. D. Rosa, F. Scarciglia, G. Buttafuoco, "Modelling seasonal variations of natural radioactivity in soils: A case study in southern Italy", *Journal of Earth System Science*, Vol. 125, No. 8, pp. 1569–1578, 2016
- [2] N. Krishnamurthy, S. Mullainathan, R. Mehra, M. A. E. Chaparro, M. A. E. Chaparro, "Radiation impact assessment of naturally occurring radionuclides and magnetic mineral studies of Bharathapuzha river sediments, South India", *Environmental Earth Sciences*, Vol. 71, No. 8, pp. 3593–3604, 2014
- [3] UNSCEAR, Sources, Effects, and Risks of Ionizing Radiation, United Nations Scientific Committee on the Effects of Atomic Radiation, 2000
- [4] S. Singh, A. Rani, R. K. Mahajan, " ^{226}Ra , ^{232}Th , and ^{40}K analysis in soil samples from some areas of Punjab and Himachal Pradesh, India using gamma-ray spectrometry", *Radiation Measurements*, Vol. 39, No. 4, pp. 431–439, 2005
- [5] R. Mehra, S. Singh, K. Singh, R. Sonkawade, " ^{226}Ra , ^{232}Th , and ^{40}K analysis in soil samples from some areas of Malwa region, Punjab, India using gamma ray spectrometry", *Environmental Monitoring and Assessment*, Vol. 134, No. 1-3, pp. 333, 2007
- [6] F. Ahmed, H. A. Shousha, H. M. Diab, "Comparative study of natural radioactivity concentrations in soil samples from the newly developed Tushki and Giza regions in Egypt", *Radiation Effects & Defects in Solids*, Vol. 161, No. 4, pp. 257–266, 2006
- [7] M. C. Bede, A. A. Essiett, E. Inam, "An assessment of absorbed dose and radiation hazard index from natural radioactivity in soils from Akwa Ibom State, Nigeria", *International Journal of Science and Technology*, Vol. 4, No. 3, pp. 80–92, 2015

- [8] S. Harb, A. H. E. Kamel, A. M. Zahran, A. Abbady, F. Ahmed, "Assessment of natural radioactivity in soil and water samples from Aden governorate South Of Yemen region", *International Journal of Recent Research in Physics and Chemical Sciences*, Vol. 1, pp. 1–7, 2014
- [9] A. M. Umar, M. Y. Onimisi, S. A. Jonah, "Baseline measurement of natural radioactivity in soil, vegetation and water in the industrial district of the federal capital territory (FCT) Abuja, Nigeria", *British Journal of Applied Science & Technology*, Vol. 2, No. 3, pp. 266–274, 2012
- [10] G. O. Awwiri, J. C. Osimobi, E. O. Agbalagba, "Evaluation of radiation hazard indices and excess lifetime cancer risk due to natural radioactivity in soil profile of Udi and Ezeagu local government areas of Enugu State, Nigeria", *Comprehensive Journal of Environmental and Earth Sciences*, Vol. 1, pp. 1–10, 2012
- [11] M. Hassan, J. S. Karniliyus, J. M. Egicya, "Radioassay of geregu soil north-central Nigeria", *Academic Research International*, Vol. 5, No. 4, pp. 69-78, 2014
- [12] G. Bouhila, F. Benrachi, M. Ramdhane, "Evaluation of natural radioactivity and assessment of radiation hazard indices in some sediment samples from streams of east Algeria", *International Journal of Nuclear and Radiation Science and Technology*, Vol. 1, pp. 7–11, 2016
- [13] Google earth V 7.3.2.5776, "Wadi Arar, Saudi Arabia", Eye alt 19.24 km, Landsat, Copernicus, <http://www.earth.google.com>, 2016
- [14] M. A. M. Alghamdi, H. M. Diab, "Measurement of radon content in silty sand soil using rad7 and Cr-39 techniques at Wadi Arar, Saudi Arabia: Comparison study", *International Journal of Management and Applied Science*, Vol. 2, No. 5, pp. 2394–7926, 2016
- [15] M. A. M. Alghamdi, "Relationship between grain size distribution and radon content in surficial sediments of Wadi Arar, Saudi Arabia", *Engineering, Technology & Applied Science Research*, Vol. 8, No. 1, pp. 2447-2451, 2018
- [16] F. Alshahri, "Radioactivity of ^{226}Ra , ^{232}Th , ^{40}K , and ^{137}Cs in beach sand and sediment near to desalination plant in eastern Saudi Arabia: Assessment of radiological impacts", *Journal of King Saud University–Science*, Vol. 29, No. 2, pp. 174–181, 2017
- [17] S. H. Q. Hamidalddin, "Measurements of the natural radioactivity along red sea coast (south beach of Jeddah Saudi Arabia)", *Life Science Journal*, Vol. 10, No. 1, pp. 121–128, 2013
- [18] H. A. A. Trabulsy, A. E. M. Khater, F. I. Habbani, "Radioactivity levels and radiological hazard indices at the Saudi coast line of the Gulf of Aqaba", *Radiation Physics and Chemistry*, Vol. 80, No. 3, pp. 343–348, 2011
- [19] A. S. Alaamer, "Measurement of natural radioactivity in sand samples collected from Ad-Dahna desert in Saudi Arabia", *World Journal of Nuclear Science and Technology*, Vol. 2, No. 4, pp. 187–191, 2012
- [20] A. F. A. Khattabi, S. M. Dini, C. A. Wallace, A. S. Banakhar, M. H. A. Kaff, A. M. A. Zahrani, *Geological Map of the Arar Quadrangle*, Saudi Geological Survey, 2010
- [21] T. Vidmar, "EffTran-A Monte Carlo efficiency transfer code for gamma-ray spectrometry", *Nuclear Instruments and Methods in Physics Research Section A: Accelerators, Spectrometers, Detectors and Associated Equipment*, Vol. 550, No. 3, pp. 603–608, 2005
- [22] T. Vidmar, N. Celik, N. C. Diaz, A. Dlabac, I. O. B. Ewa, J. A. C. Gonzalez, M. Hult, S. Jovanovic, M. C. Lepy, N. Mihaljevic, O. Sima, F. Tzika, M. J. Vargas, T. Vasilopoulou, G. Vidmar, "Testing efficiency transfer codes for equivalence", *Applied Radiation and Isotopes*, Vol. 68, No. 2, pp. 355–359, 2010
- [23] T. Vidmar, G. Kanisch, G. Vidmar, "Calculation of true coincidence summing corrections for extended sources with EffTran", *Applied Radiation and Isotopes*, Vol. 69, No. 6, pp. 908–911, 2011
- [24] R. Veiga, N. Sanches, R. M. Anjos, K. Macario, J. Bastos, M. Iguatemy, J. G. Aguiar, A. M. A. Santos, B. Mosquera, C. Carvalho, M. B. Filho, N. K. Umisedo, "Measurement of natural radioactivity in Brazilian beach sands", *Radiation measurements*, Vol. 41, No. 2, pp. 189–196, 2006
- [25] H. M. Diab, S. A. Nouh, A. Hamdy, S. A. E. Fiki, "Evaluation of natural radioactivity in a cultivated area around a fertilizer factory", *Journal of Nuclear and Radiation Physics*, Vol. 3, No. 1, pp. 53–62, 2008
- [26] European Commission, Radiation Protection 112, *Radiological Protection Principles Concerning the Natural Radioactivity of Building Materials*, European Commission, Office for Official Publications of the European Communities, 1999
- [27] M. A. M. Alghamdi, "Grain size distribution and mineral composition of surficial quaternary sediments of Wadi Arar, Saudi Arabia", *International Journal of Advances in Science Engineering and Technology*, Vol. 6, No. 1, pp. 40–43, 2018
- [28] M. A. M. Alghamdi, A. A. E. Hegazy, "Physical properties of soil sediment in Wadi Arar, Kingdom of Saudi Arabia", *International Journal of Civil Engineering*, Vol. 2, pp. 1-8, 2013